International Journal of Minerals, Metallurgy and Materials

International Journal of Minerals, Metallurgy and Materials

Volume 14 | Issue 7 Article 16

June 2007

Plastic deformation behavior of $Fe_{40}Ni_{40}P_{14}B_6$ bulk metallic glass investigated by nanoindentation

Changqing Zhang
Key Laboratory for Advanced Manufacturing by Materials Processing Technology, Department of Mechanical Engineering, Tsinghua University, Beijing 100084, China

Kefu Yao
Key Laboratory for Advanced Manufacturing by Materials Processing Technology, Department of Mechanical Engineering, Tsinghua University, Beijing 100084, China

Recommended Citation

Zhang Changqing, Yao Kefu. Plastic deformation behavior of $Fe_{40}Ni_{40}P_{14}B_6$ bulk metallic glass investigated by nanoindentation, *Int. J. Miner. Metall. Mater.,* 14 (2007), No. 7, Article 16, p. 68-72.

Journal of University of Science and Technology Beijing
Volume 14, Supplement 1, June 2007, Page 68

Materials

Plastic deformation behavior of $Fe_{40}Ni_{40}P_{14}B_6$ bulk metallic glass investigated by nanoindentation

Changqing Zhang and Kefu Yao

Key Laboratory for Advanced Manufacturing by Materials Processing Technology, Department of Mechanical Engineering, Tsinghua University, Beijing 100084, China

(Received 2006-06-16)

Abstract: $Fe_{40}Ni_{40}P_{14}B_6$ bulk metallic glass rods have been prepared by water quenching the fluxed alloy. The deformation behavior was investigated by nanoindentation tests and compressing tests. The average hardness and elastic modulus of the as-prepared $Fe_{40}Ni_{40}P_{14}B_6$ BMG (bulk metallic glass) measured by nanoindentation tests are 8.347 and 176.61 GPa respectively. The displacement-load curve shows "pop-in" characteristics which correspond to the loading rate bursts. Many shear bands around the indent were observed. The as-prepared Fe-based BMG exhibits a compressive plastic strain of 5.21%, which is much larger than that of other Fe-based glassy alloys and most of other BMGs.

Key words: $Fe_{40}Ni_{40}P_{14}B_6$ bulk metallic glass; nanoindentation tests; compressing tests, "pop-in" characteristics, shear bands, compressive plastic strain

1. Introduction

In the past two decades, nanoindentation tests were widely used in measuring the materials' hardness and elastic modulus [1-3]. Recently nanoindentation tests have been proposed as an important tool for studying fundamental physics of deformation in metallic glasses by Wright *et al.* [4] and Golovin *et al.* [5], such as identifying the rate effect on serrated flow behavior, discrete plasticity and structural change beneath the indenter *etc.* By using instrumented indentation, many studies on serrated flow behavior and its strain rate-dependence in amorphous metals, such as in Pd- [5-8], Zr- [6-10], La- [9], Al- [11], Fe- [12], Ni- [13] and Nd-based alloys [14], have clearly shown that pop-in and/or discrete displacement burst events appear in the load-indentation depth curve when the loading rate is very low. In contrast, as the rate is increased the pop-in events are gradually suppressed and even disappear. W.J. Wright *et al.* have first developed a complementary analysis to extract the strength of a Mohr-Coulomb solid from the *P-h* (load-displacement) data of the first pop-in [4]. Vaidyanathan *et al.* combined finite element modeling with instrumental indentation to assess the yield criterion of a Zr-based BMG [15]. Many shear bands were observed on the surface around the indentations in metallic glasses and they were recognized as the contours of maximum shear deformation beneath a Berkovich indenter [15]. There were a few experimental studies revealed the shape of the flow field beneath the indenter by macroscopic observations [16-17] and also revealed details of atomic-scale structural change such as nanocrystallization or medium-range ordering beneath an indentation [18-19] by transmission electron microscopy (TEM) observations. Bei *et al.* determined the theoretical shear strengths of the BMGs through investigating their mechanical behavior by nanoindentation with a spherical indenter [20]. Very recently, B. Yang *et al.* observed strain hardening and recovery phenomenon in a $Zr_{52.5}Cu_{17.9}Ni_{14.6}Al_{10.0}Ti_{5.0}$ glassy alloy using a controlled instrumented nanoindentation technique [21]. So nanoindentation experiments plays an important role in elucidating the fundamental mechanisms of plasticity in metallic glasses.

The $Fe_{40}Ni_{40}P_{14}B_6$ glassy alloy (also called as Metglas 2826) is an excellent soft magnetic material [22]. But only a glassy alloy ribbon can be prepared for a long time due to its lower glass forming ability (GFA). In 2001, a 1-mm diameter $Fe_{40}Ni_{40}P_{14}B_6$ BMG rod was successfully made by T.D. Shen and R.B. Schwarz through fluxing and water-quenching technique [23]. We successfully prepared $Fe_{40}Ni_{40}P_{14}B_6$ BMG rods (1.6 mm in diameter) with good plasticity, and utilized nanoindentation and uniaxial compression experiments to investigate the mechanical properties of $Fe_{40}Ni_{40}P_{14}B_6$ BMG.

Corresponding author: Kefu Yao, **E-mail:** kfyao@tsinghua.edu.cn

2. Experimental

The $Fe_{40}Ni_{40}P_{14}B_6$ alloy (whose composition is given in nominal atomic percentages) ingots were prepared by induction-melting a mixture of Ni (99.95 wt% in purity), B (99.999wt% in purity), Ni_2P (99.5wt% in purity) powders and Fe (99.98wt% in purity) grains in a purified argon atmosphere. The fluxing technique has been used to purify the alloy. The alloy samples were put into the B_2O_3 melt under vacuum condition and kept at 1430 K for about 10 h. Then the purified alloy samples were re-melted in a quartz tube under vacuum condition and quenched in water. The structure of the as-quenched samples were characterized by X-ray diffraction (XRD) using a Rigaku D/max-RB diffractometer with monochromatic CuK_α radiation. The microstructures of the as-prepared alloys were also examined by use of a JEM-200CX transmission electron microscope (TEM). The thin foil specimens were prepared by twin-jet electropolishing method. The Vickers hardness was determined under a load of 200 g by an MH-3 hardness tester. Nanoindentation experiments were conducted at room temperature using a Nanoindenter XP (Nano Instruments Innovation Center, MTS Corporation, Knoxville, TN) with a Berkovich diamond indenter at a constant strain rate of 0.05 s^{-1}. The morphology of the surface was observed using a LEO-1530 scanning electron microscope installed a field emission gun.

3. Results and discussion

Fig. 1 shows the XRD spectrum of the as-prepared specimens, except the broad diffraction peak, no sharp diffraction peak corresponding to crystalline structure can be observed, indicating that the as-quenched alloy rods with 1.6 mm in diameter possesses amorphous structure. It shows that the GFA of the alloy has been significantly enhanced after fluxing, agreed with the reported results [23-27]. The thin foil specimens had been carefully examined with TEM, no crystalline phase had been found. The insert of Fig. 2 is the selected area electron diffraction (SAED) pattern, showing only diffuse halos corresponding to amorphous structure. Fig. 2 further confirms the homogeneous amorphous structure of the alloys.

The plastic deformation behavior of $Fe_{40}Ni_{40}P_{14}B_6$ BMG by nanoindentation was studied. Typical load-displacement (P-h) curves of nanoindentation tests are presented in Fig. 3. The BMG was indented to a maximum depth of 1500 nm because the measured hardness reaches stable value at the depth larger than 1000 nm (see Fig. 4(b)). The test was carried out at a constant strain rate of 0.05 s^{-1}. The unloading curve reflects the elastic behavior and the loading curve shows the elastoplastic behavior of the material. The inset of Fig. 3 shows that the loading curve displays discrete steps or 'pop-in' events indicating the sudden penetration of the indenter tip into the sample, and these serrations correspond to the activation of individual shear bands [8].

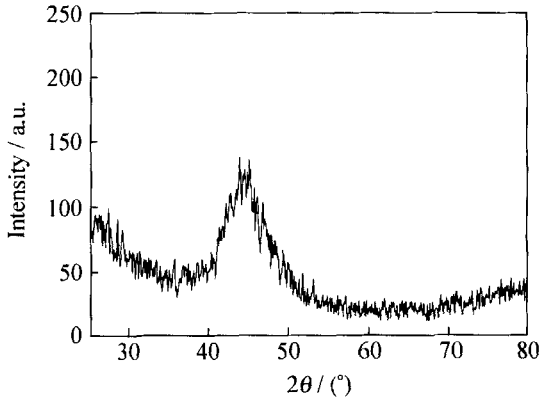

Fig. 1. XRD pattern of $Fe_{40}Ni_{40}P_{14}B_6$ bulk metallic glass.

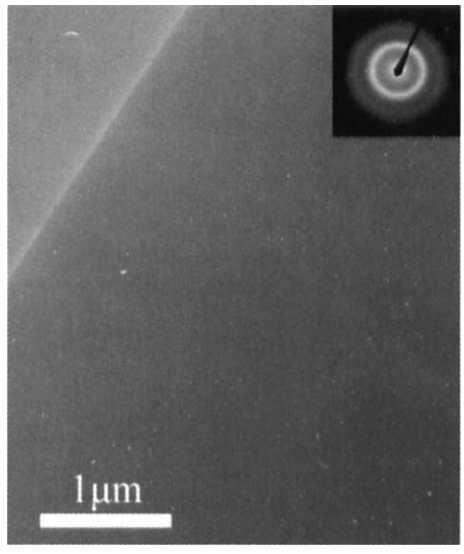

Fig. 2. TEM image of $Fe_{40}Ni_{40}P_{14}B_6$ metallic glass. The inset is the selected area electron diffraction (SAED) pattern.

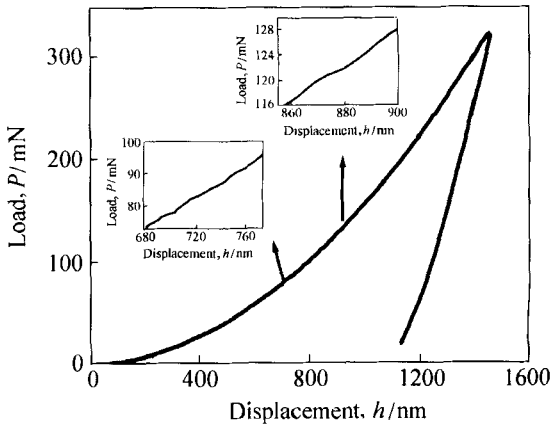

Fig. 3. Typical load-displacement (P-h) curves of $Fe_{40}Ni_{40}P_{14}B_6$ BMG by nanoindentation experiments.

Hardness and elastic modulus profiles as a function of indentation depth for the alloys are shown in Fig. 4. It shows that the modulus basically keeps constant at different depths. While the hardness falls gradually as the indent proceeds and tends to be a constant. The measured average hardness and modulus of the $Fe_{40}Ni_{40}P_{14}B_6$ BMG are 8.347 and 176.61 GPa, respectively. Generally, the measured hardness value is directly proportional to the material's yield which is expressed by Tabor as $H=K\cdot\sigma_y$ [28], where H is the hardness, σ_y is the yield strength, K is a constant and for amorphous metals the value of K is about 3. The σ_y of $Fe_{40}Ni_{40}P_{14}B_6$ BMG is about 2.23 GPa [29], so the value of K is about 3.7 which is bigger than the empirical value. The reason of the glassy alloy with higher K is not clear.

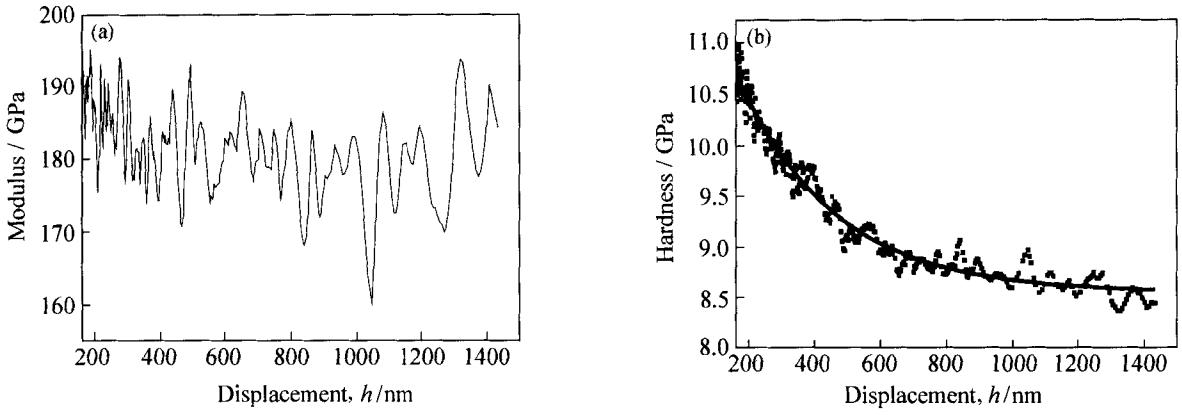

Fig. 4. Elastic modulus (a) and hardness (b) profiles as a function of indentation depth.

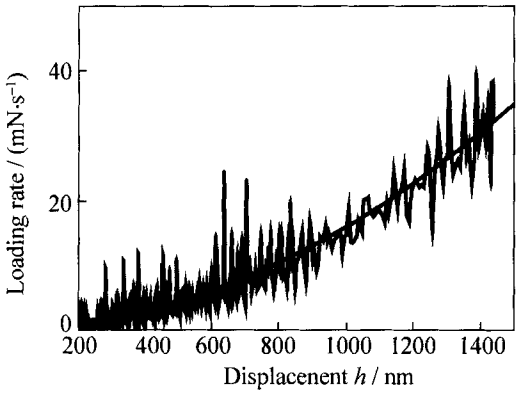

Fig. 5. Loading rate changes as a function of displacement.

During nanoindentation at a constant strain rate, the loading rate can be expressed as $dP/dt=\dot{\varepsilon}h dP/dh$ [8], where dP/dt is the loading rate, $\dot{\varepsilon}$ is the strain rate, h is the displacement or the depth. The loading rate is plotted as a function of displacement in Fig. 5. As Fig. 5 illustrates, with the increase of displacement, the loading rate is not monotonic increase, there are many short peaks in loading rate and their occurrence frequency decreases gradually. If examining Fig. 5 carefully, it can be found that the height of the peaks at different displacement is different. When h<900 nm, the peaks range of loading rate is about 10 mN/s. When 900 nm≤h≤1150 nm, the peaks range is about 5 mN/s. While for h>1150 nm, it is about 18 mN/s. These peaks are found to correspond exactly with the "pop-in" events in Fig. 3. Correspondingly, the discrete displacement in the P-h curves of Fig. 3 also reduces as the loading rate increases. So the serrations flow is related to the loading rate during nanoindentation at a constant strain rate. At a higher load, the width of discrete displacement is wider than that at a lower load, the reason is that the length scale of the indentation geometry increases as the depth increases.

Fig. 6(a) is a SEM image of indent feature of $Fe_{40}Ni_{40}P_{14}B_6$ BMG alloy. Fig. 6(b) is the high magnification image of Fig. 6(a). As shown in Fig. 6, many pile-up shear traces around the indent can be observed and no microcrack has been observed around the indent.

When the metallic glass is indented by Berkovich diamond indenter, its deformation can be classified to two stages: the elastic deformation stage and the elastoplastic deformation stage. The elastic deformation occurs first. With the indent depth increases, the BMG yields and demonstrates the first pop-in event at the load-displacement curves. Simultaneously, the material turns into elastoplastic deformation period. The plastic deformation region around the indenter is constrained by the surrounding elastic material which suppressing the unstable extension of dominant shear bands. So the shearing deformation is highly localized. The plastic deformation takes place in the area beneath the indenter, many shear bands form which correlated with the strain serrations. The formation of shear bands is determined by local arrangements of atoms, the local free volume as well as short- or medium-range ordering of the local constituents [9, 19] and it is also related to the local deformation history [9,

19].

The Vickers hardness of $Fe_{40}Ni_{40}P_{14}B_6$ BMG is 7.22 GPa, which is smaller than that measured by nanoindentation. The reason is that the measurement method is different between the Vickers hardness and nanoindentation tests. In Vickers hardness tests, the size of the residual impression in the surface is used to determine the hardness value. But in nanoindentation tests, the size of the contact area under full load is determined from the depth of penetration of the indenter and the shape of the elastic recovery during removal of load, it provides an estimate of the area of the contact under full load [30].

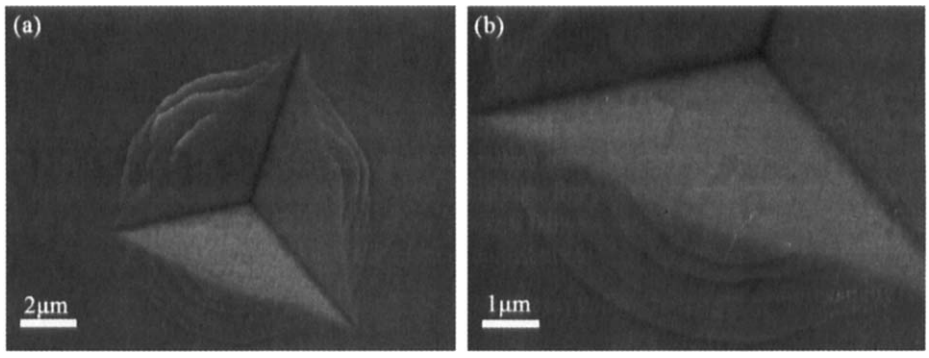

Fig. 6. (a) SEM image of localized plastic flow around a Berkovich indent on the surface of $Fe_{40}Ni_{40}P_{14}B_6$ BMG; (b) magnification of (a).

The room-temperature uniaxial compression tests were carried out on an Instron-type testing machine at a strain rate of 3×10^{-4} s^{-1}. The yield strength of the glassy alloy is about 2.23 GPa, which is similar to the reported value (2.1-2.4 GPa) of $Fe_{40}Ni_{40}P_{14}B_6$ glassy ribbon [31-32]. The measured compressive plastic strain of the BMG is about 5.21%, which is much larger than that of most BMGs (which plastic strain is usually less than 2%). Due to the length limitation, the details of the compress testing result will be reported elsewhere. The present result demonstrates that the plasticity of pure Fe-based glassy alloys can be extensively improved, which is meaningful for developing BMGs and for their applications.

4. Conclusions

(1) The $Fe_{40}Ni_{40}P_{14}B_6$ bulk metallic glass rods of 1.6 mm in diameter have been prepared by fluxing and water quenching method. The GFA of this alloy is greatly enhanced by this method.

(2) The measured average hardness and the elastic modulus of the as-prepared $Fe_{40}Ni_{40}P_{14}B_6$ BMG are 8.347 and 176.61 GPa respectively by nanoindentation tests. Shear traces around the indent were observed and no microcrack around the indent has been observed.

(3) The "pop-in" phenomenon in *P-h* curves is related to a series of discrete loading rate changes. During nanoindentation tests at constant strain rates, the frequency of loading-rate change peaks is much larger at small depth. And it decreases with the increase of indent depth.

(4) The as-prepared Fe-based BMG exhibits a compressive plastic strain of 5.21%, which is much larger than that of most BMGs.

References

[1] W.C. Oliver and G.M. Pharr, Improved technique for determining hardness and elastic modulus using load and displacement sensing indentation experiments, *J. Mater. Res.*, 7(1992), p.1564.

[2] W.C. Oliver and G.M. Pharr, Measurement of hardness and elastic modulus by instrumented indentation: Advances in understanding and refinements to methodology, *J. Mater. Res.*, 19(2004), p.3.

[3] B. Bhushan, *In Handbook of Micro/Nano Tribology*, CRC Press, Florida, 1999, p.433.

[4] W.J. Wright, R. Saha, and W.D. Nix, Deformation mechanisms of the $Zr_{40}Ti_{14}Ni_{10}Cu_{12}Be_{24}$ bulk metallic glass, *Mater. Trans. JIM*, 42(2001), p.642.

[5] Y.I. Golovin, V.I. Ivolgin, V.A. Khonik, *et al.*, Serrated plastic flow during nanoindentation of a bulk metallic glass, *Scripta Mater.*, 45(2001), p.947.

[6] C.A. Schuh, T.G. Nieh, and Y. Kawamura, Rate dependence of serrated flow during nanoindentation of a bulk metallic glass, *J. Mater. Res.*, 17(2002), p.1651.

[7] C.A. Schuh, A.S. Argon, T.G. Nieh, *et al.*, The transition from localized to homogeneous plasticity during nanoindentation of an amorphous metal, *Philos. Magn.*, 83(2003), p.2585.

[8] C.A. Schuh and T.G. Nieh, A nanoindentation study of serrated flow in bulk metallic glasses, *Acta Mater.*, 51(2003), p.87.

[9] T.G. Nieh, C.A. Schuh, J. Wadsworth, *et al.*, Strain rate-dependent deformation in bulk metallic glasses, *Intermetallics*, 10(2002), p.1177.

[10] L. Liu and K.C. Chan, Plastic deformation of Zr-based bulk metallic glasses under nanoindentation, *Mater. Lett.*,

59(2005), p.3090.

[11] W.H. Jiang and M. Atzmon, Rate dependence of serrated flow in a metallic glass, *J. Mater. Res.*, 18(2003), p.755.

[12] A.L. Greer and I.T. Walker, Transformations in primary crystallites in (Fe,Ni)-based metallic glasses, *Mater. Sci. Forum*, 386-388(2002), p.77.

[13] A.L. Greer, A. Castellero, S.V. Madge, *et al.*, Nanoindentation studies of shear banding in fully amorphous and partially devitrified metallic alloys, *Mater. Sci. Eng. A*, 375-377(2004), p.1182.

[14] B.C. Wei, T.H. Zhang, W.H. Li, *et al.*, Serrated plastic flow during nanoindentation in Nd-based bulk metallic glasses, *Intermetallics*, 12(2004), p.1239

[15] R. Vaidyanathan, M. Dao, G. Ravichandran, *et al.*, Study of mechanical deformation in bulk metallic glass through instrumented indentation, *Acta Mater.*, 49(2001), p.3781.

[16] P.E. Donovan, Plastic flow and fracture of $Pd_{40}Ni_{40}P_{20}$ metallic glass under an indentor, *J. Mater.Sci.*, 24(1989), p.523.

[17] U. Ramamurty, S. Jana, Y. Kawamura, *et al.*, Hardness and plastic deformation in a bulk metallic glass, *Acta Mater.*, 53 (2005), p.705.

[18] J.J. Kim, Y. Choi, S. Suresh, *et al.*, Nanocrystallization during nanoindentation of a bulk amorphous metal alloy at room temperature, *Science*, 295(2002), p.654.

[19] C.A. Schuh and T.G. Nieh, A survey of instrumented indentation studies on metallic glasses, *J. Mater. Res.*, 19(2004), p.46.

[20] H. Bei, Z.P. Lu, and E.P. George, Theoretical strength and the onset of plasticity in bulk metallic glasses investigated by nanoindentation with a spherical indenter, *Phys. Rev. Lett.*, 17(2004), p.125504.

[21] B. Yang, L. Riester, and T.G. Nieh, Strain hardening and recovery in a bulk metallic glass under nanoindentation, *Scripta Mater.*, 54(2006), p.1277.

[22] F.E. Luborsky, J.J. Becker, and R.O. McCary, Magnetic annealing of amorphous alloys, *IEEE Trans. Magn.*, MAG-11(1975), p.1644.

[23] T.D. Shen and R.B. Schwarz, Bulk ferromagnetic glasses in the Fe-Ni-P-B system, *Acta Mater.*, 49(2001), p.837.

[24] K.F. Yao and F. Ruan, Pd-Si binary bulk metallic glass prepared at low cooling rate, *Chin. Phys. Lett.*, 22(2005), p.1481.

[25] K.F. Yao, F. Ruan, Y.Q. Yang, *et al.*, Superductile bulk metallic glass, *Appl. Phys. Lett.*, 88(2006), p.122106

[26] A. Inoue, Stabilization of metallic supercooled liquid and bulk amorphous alloys, *Acta Mater.*, 48(2000), p.279.

[27] W.L. Johnson, Bulk glass-forming metallic alloys: Science and technology, *MRS Bull.*, 24(1999), p.42.

[28] D. Tabor, *The Hardness of Metals*, Clarendon Press, London, 1951.

[29] K.F. Yao and C.Q. Zhang, A Fe-based bulk glasses with high plasticity, *Appl. Phys. Lett.*, 90(2007), p.061901.

[30] A.C. Fischer-Cripps, *Nanoindentation*, Springer Press, New York, 2002, p.23.

[31] D.J. Krenitsky and D.G. Ast., Temperature dependence of the flow stress and ductility of annealed and unannealed amorphous $Fe_{40}Ni_{40}P_{14}B_6$, *J. Mater. Sci.*, 14(1979), p.275.

[32] D.G. Ast and D.J. Krenitsky, Fracture toughness and yield strength of annealed Ni EM DASH Fe base metallic glasses, *Mater. Sci. Eng.*, 23(1975), p.241.